

## MEASURING CURRENT DISCHARGE STORED ENERGY IN CAPACITORS WELDING

Victor POPOVICI<sup>1\*</sup>, Delicia ARSENE<sup>2</sup>, Claudia BORDA<sup>3</sup>

<sup>1)</sup> Assoc. Prof., PhD, Materials Technology and Welding Department, University “Politehnica” of Bucharest, Romania

<sup>2)</sup> Lecturer, PhD, Materials Technology and Welding Department, University “Politehnica” of Bucharest, Romania

<sup>2)</sup> Lecturer, PhD, Materials Technology and Welding Department, University “Politehnica” of Bucharest, Romania

**Abstract:** This paper presents an alternative for measuring the discharge current welding with stored energy in capacitors. Spot welding equipment with stored energy electrostatic allow very harsh regimes that ensure very short times and high currents. These regimes welding allow precise metering of energy at welds and heat concentration in the desired region. Welding stored energy in capacitors is applied to welding materials and alloys with high thermal conductivity, welding special steels, where thermal cycling tough being put steel in the short time of welding restrict minimal heat affected zone and does not lead to formation of structures fragile at welding materials and alloys of different nature which occurs at the point where alloy weld is very small homogeneous. In the case of thin parts at the welding energy cannot be dispensed to produce apertures. The discharge current measurement (kA) in phase can be done with a coil-type transducer Rogowski. Magnetomotive voltage provided by the Rogowski coil is taken by an integrator amplifier circuit. Chain calibration is shown for measuring the discharge current using Rogowski coil transducer and the experimental results regarding the variation of discharge currents according to the charging voltage and stored energy equipment and without turned to welding. Experiments are presented on the phenomenon of welding transformer core saturation. Disclosed is a method for measuring current discharge stored energy welding using a Hall transducer.

**Key words:** discharge current, stored energy in capacitors, weld current measurement, Rogowski coil.

### 1. INTRODUCTION

Pressure welding is a welding process that ensures a good quality welded joints with high productivity.

In the spot welding process, two overlapped components are welded together as a result of the resistance heating caused by the passage of electric current.

This resistance heating is provided by the workpieces as they are held together under pressure between two electrodes as shown in Fig. 1 [1].

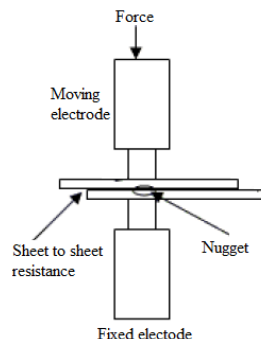


**Fig.1.** The occurrence of resistances in electrical resistance spot welding.

The electrodes used in applying pressure and transmission of electric current through the parts to form the nugget are copper (brass) core length of tungsten thorium free zero.

The magnitude and duration of the current and the resistance of the workpieces determine the size of the formed nugget.

Figure 2 presents two device port-electrodes enforcement and pneumatic pressure control.

Welding supply (Joule-Lenz effect) problem is achieving very harsh regimes that ensure very short times and high currents.

This can be achieved using welding equipment in points with stored energy electrostatic field.

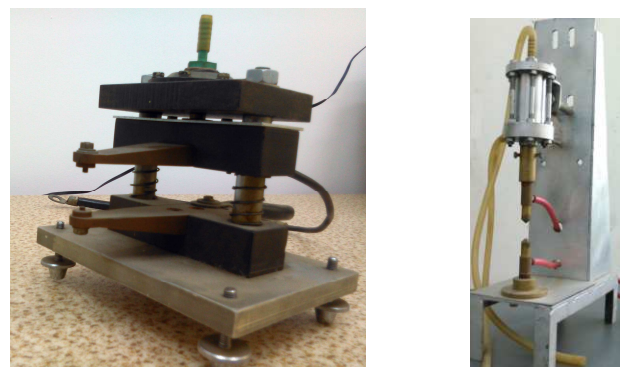


**Fig. 2.** Device port-electrodes pneumatic pressure control.

\* Corresponding author: Splaiul Independenței 313, sector 6, 060042, Bucharest, Romania, Tel.: 0040 727 442 933 E-mail addresses: popovici\_victor@yahoo.com (V. Popovici)

Spot welding equipment with stored energy electrostatic field enables precise metering of energy at welds and heat concentration in the desired region in a very short time.

It saves electricity because charging the battery energy (capacitors) requires low power to the grid, this relatively long loading time due to the time of discharge capacitors (of the order of microseconds).

By reducing the heating time and increasing the level of heat source heat loss is reduced to the maximum.

Welding stored energy can be applied to welding materials and alloys with high thermal conductivity.

Special steel welding heat cycle that undergoes tough in the short time of welding steel restrict to a minimum the heat affected zone and does not lead to the formation of brittle structures.

Welding materials and alloys of different nature which occurs at the point welded alloy is very small and thus the size is homogeneous.

Thin pieces at the weld energy can be given to not produce breakthroughs.

When welding point stored energy in capacitors is recommended that copper electrodes (brass) contain a core of thorium wolfram free zero length.



Fig. 3. The microstructure of the weldment stored energy of a copper wire with a diameter of 0.1 on a silver foil with a thickness of 0.1 mm.

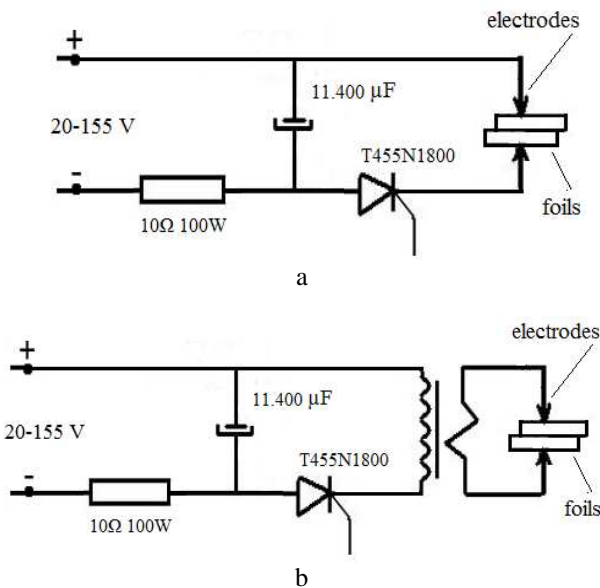


Fig.4. Principle scheme of the spot welding with stored energy in capacitors: a – direct discharge; b – discharge welding transformer.

Figure 3 shows the microstructure of the weldment stored energy in capacitors of a copper wire with a diameter of 0.1 on a silver foil with a thickness of 0.1mm.

Schematic diagram of spot welding equipment stored energy in capacitors is shown in Fig. 4.

Figure 4,a shows a drawing of welding equipment with stored energy in capacitors with direct discharge and loading scheme in Fig. 4,b welding transformer.

## 2. WELDING CURRENT MEASUREMENT

### 2.1. Rogowski coil

Given the transitory nature and high values of the discharge current kA can use a Rogowski coil transducer.

Rogowski coil consists of a flexible tube of constant section, small enough to be considered a uniform magnetic field in a given section.

It is the inductor uniform, turn beside turn, winding a thin insulated wire  $n_0$  turns per unit length.

The coil is then placed around conductors whose currents are to be measured (Fig. 5).

As Rogowski coils use a non-magnetic core to support the secondary windings, mutual coupling between the primary and secondary windings is weak.

Because of weak coupling, to obtain quality current sensors, Rogowski coils should be designed to meet two main criteria: the relative position of the primary conductor inside the coil loop should not affect the coil output signal; the impact of nearby conductors that carry high currents on the coil output signal should be minimal.

To satisfy the first criteria, mutual inductance  $M$  must have a constant value for any position of the primary conductor inside the coil loop.

Mutual inductance  $M$  is defined by the formula:

$$M = \mu_0 \cdot n \cdot S, \tag{1}$$

where  $\mu_0$  is permeability of air.

Because the Rogowski coil primary and secondary windings are weakly coupled (to prevent the unwanted influence from nearby conductors carrying high currents) Rogowski coils are designed with two wire loops connected in electrically opposite directions.

This cancels electromagnetic fields coming from outside the coil loop.

One or both loops can consist of wound wire. If only one loop is constructed as a winding, then the second

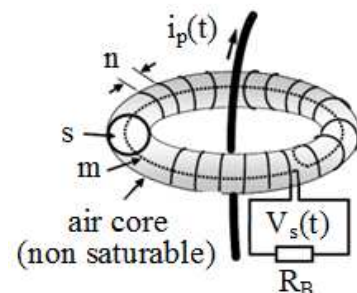


Fig. 5. Rogowski coil [2].

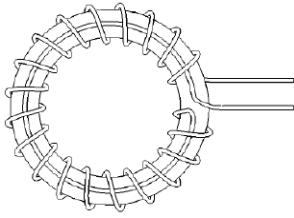


Fig. 6. Rogowski coil with the return wire loop through the winding.

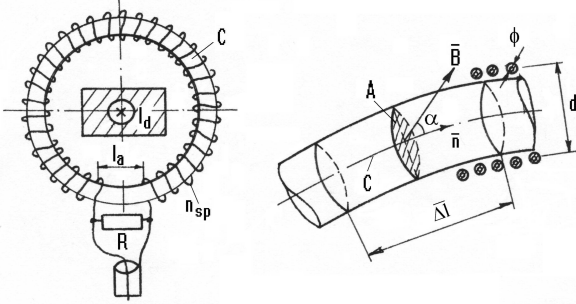


Fig. 7. Rogowski coil construction elements.

wire loop can be constructed by returning the wire through (Fig. 6) or near this winding (single-layer coils).

If both loops are constructed as windings, then they must be wound in opposite directions (multi-layer coils).

In this way, the Rogowski coil output voltage induced by currents from the inside conductor(s) will be doubled if windings are identical.

The ends of the winding are connected to an integrator voltage amplifier circuit.

For the measurement of the welding current average fibre Rogowski coil will be circular.

Rogowski coil average fibre may have a circular shape.

Rogowski coil construction elements are (Fig. 7): the diameter of the curve  $C = \Phi 30$  mm; the winding diameter  $d = \Phi 4.6$  mm;  $\Phi 0.6$  mm wire diameter; number of turns  $n_0 = 125$ ; non wirewound land length  $l_0 = 10$  mm;  $R =$  resistance 130  $\Omega$ .

For a portion of the coil length  $\Delta l$  small enough to be considered the same magnetic flux  $\Phi_s = \bar{B}ndA$   $n_0\Delta l$  through each of the coils contained therein, the total flow is:

$$n_0\Delta l \phi = n_0 \mu_0 \overline{AHnl} = n_0 \mu_0 \overline{AH} \Delta l. \quad (2)$$

Total magnetic flux through the coil winding is:

$$\Phi = n_0 \mu_0 A \Delta \bar{H} l = n_0 \mu_0 A \sum \bar{H} d\bar{l} = k_R U_{mC}. \quad (3)$$

The tension  $U_{mC}$  along the curve  $C$  axis magnetic coil is

$$U_{mC} = \int_C \bar{H} d\bar{l} \quad (4)$$

and the coil is constant  $k_R = \mu_0 n_0 A$ .

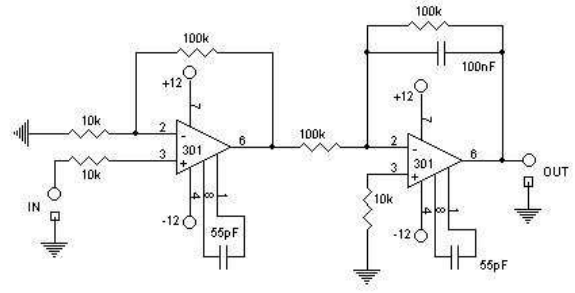


Fig. 8. Wiring diagram of the amplifier and the integrator voltage.

Constant  $k_R$  can be determined knowing the design data  $n$ ,  $l$ , and  $d$ , using the relationship:

$$k_R = \mu_0 \frac{n \pi}{l} d^2. \quad (5)$$

The ends of the winding are connected to a device consisting of a voltage amplifier and an integrator.

### 2.2. Integrated amplifier

Voltage provided by the magnetomotive force is taken up by a Rogowski coil circuit consists of an integrator followed by an amplifier (Fig. 8).

Amplifier integrator operational amplifiers were used with the offsetting of the outer LM301AN frequency.

The first floor is a voltage amplifier which receives the non-inverting input voltage magnetomotive provided Rogowski coil. The output of the amplifier is brought to the entrance integrator constant integration of 1ms.

The output of the integrator can be viewed on the oscilloscope.

### 2.3. Calibration chain for measuring the discharge current using Rogowski coil as a transducer

Calibration was performed by measuring different values of secondary currents in a welding transformer, which is responsible for resistance power adjustable in steps (Table 1).

Current measurements were made simultaneously with a measuring transformer and Rogowski coil.

The signal provided by Rogowski coil chain as measured simultaneously integrated amplifier with a digital electronic voltmeter (voltage effective) and viewed on the oscilloscope.

Table 1

Calibration chain for measuring the discharge current

Current measured measuring transformer [A]	The voltage at the output of integrator measured with the voltmeter [mV]
36	10.7
54	16.3
72	21.3
90	26.7
120	36.1
156	47.7
198	58.2
210	61.5

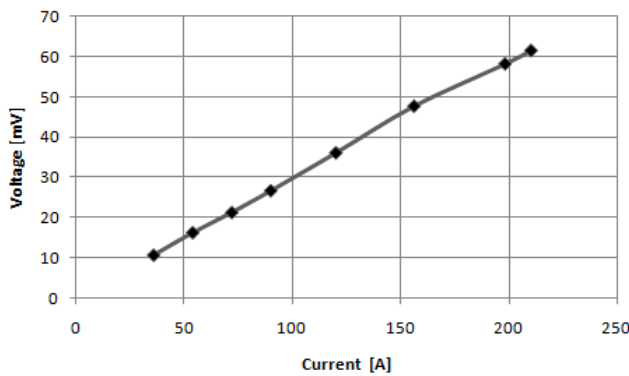


Fig. 9. Calibration.

Since pulse current discharge circuit is half-wave, comparing its amplitude is obtained on oscillogram measured value transformer with half measures.

In Fig. 9 is shown in a coordinate system: current calibration  $i_{et}$  (A) – derived from the signal integrator  $u_{int}$  ( $mv_{ef}$ ). One can find good linearity chain for measuring the discharge current.

### 3. EXPERIMENTAL RESULTS

In determining the initial discharge current ( $I_{0d}$ ) welding stored energy in capacitors, it conducted a set of measurements for the two variants of equipment with and without welding transformer.

Table 2 shows the values of the initial current discharge according to the charging voltage  $U$  [V] and the energy stored in the capacitor  $W$  [J] for welding equipment with stored energy transformerless welding  $I_{0d}$  [kA] and transformer welding  $I_{pd}$  [kA] (current measurement is made in the welding transformer primary) under the following experimental conditions:

- battery capacitors  $C = 11.400 \mu F$ ;
- tungsten thorium electrodes  $\varnothing 3$  mm cage (to ensure minimum possible contact resistance);
- welding transformer toroidal transformer ratio  $N/n = 13/7$ .

In the same experimental conditions measured discharge current  $I_{sd}$  [kA] welding transformer secondary.

Table 2

The initial current discharge according to the energy stored in the capacitor

U [V]	Energy stored in the capacitor [J]	Current discharge [kA]		
		$I_{0d}$	$I_{pd}$	$I_{sd}$
20	2.28	6.3	3	6.0
40	9.12	9	4.5	8.4
60	20.5	9.9	6	10.2
80	36.48	12.3	7.2	11.4
100	56.99	13.35	8.4	12.6
120	82.08	15.9	9.6	12.9
140	111.72	17.2	11.4	15.0
150	128.25	18.3	12.6	15.6
155	136.94	18.75	13.2	16.2

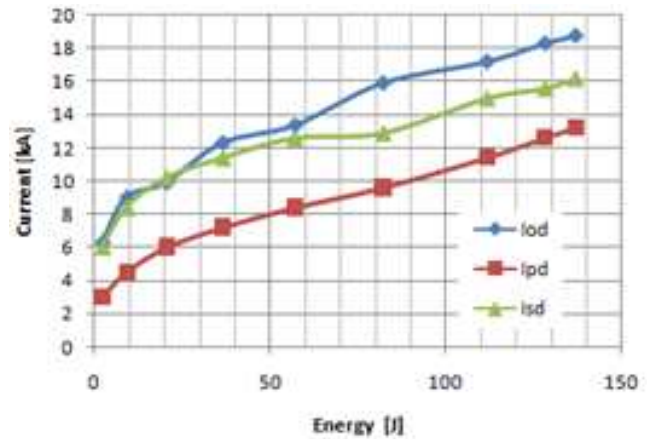


Fig. 10. Discharge current.

The variation of discharge current depending on the charging voltage and the stored energy is given in Fig. 10.

A slight increase in the discharge current, measured both in both primary and secondary transformer welding for large energy discharge phenomenon is due to transformer core saturation.

The phenomenon of saturation of the core can be better highlighted the change in the transformation ratio of the transformer welding ( $n$ ) depending on the stored energy  $W$  [J] and the discharge current in the primary,  $I_{pd}$  [kA] (Table 3, Fig. 11).

The observed decrease in the conversion ratio ( $n$ ) with increasing power.

Table 3

The phenomenon of saturation of the core

Ratio of the transformer welding $n$	Stored energy $W$ [J]	Discharge current in the primary $I_{0d}$ [kA]
2	2.28	3
1.86	9.12	4.5
1.7	20.5	6
1.58	36.48	7.2
1.5	56.99	8.4
1.34	82.08	9.6
1.31	111.72	11.4
1.23	128.25	12.6
1.22	136.94	13.2

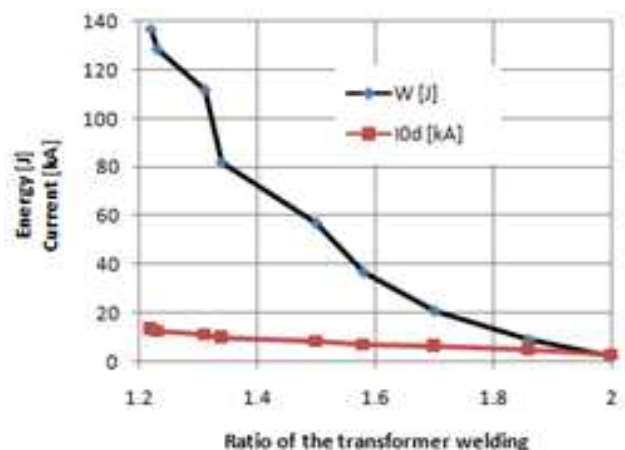
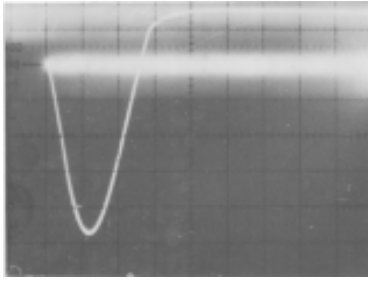


Fig. 11. The phenomenon of saturation.



**Fig. 12.** Oscillogram  $I_{0d}$  discharge current the capacitor if transformerless.

The stored energy welding equipment welding transformers are designed to increase the welding current and to protect the operator from electric shock if that does not occur discharge of the capacitor.

Experiments have shown that to obtain a current at least equal to that obtained with transformer welding equipment requires a large and expensive construction thereof (permalloy replacing the core of the ferrite core and the increase ratio of conversion).

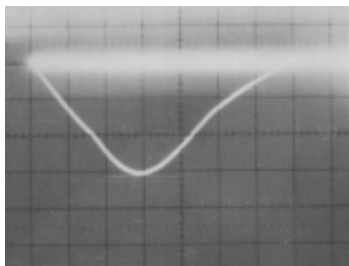
$I_{0d}$  oscillograms discharge current demonstrated influence on welding transformer welding regime parameters stored energy.

Figure 12 shows the oscillogram  $I_{0d}$  discharge current, discharge the capacitor if transformerless.

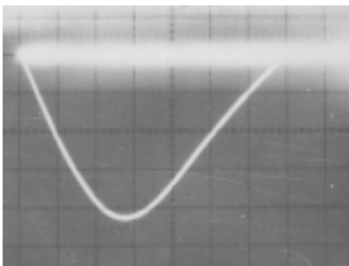
Experimental conditions:

- battery capacity  $C = 11.400 \mu\text{F}$ ;
- charging voltage  $U = 20\text{--}155 \text{ V}$ ;
- stored energy  $W = 2.26\text{--}126.94 \text{ J}$ ;
- thorium tungsten electrodes  $\Phi 3 \text{ mm}$  cage.

In Fig. 13,*a* and 13,*b* oscillograms of the discharge current in the transformer primary  $I_{0d}$  welding (Fig. 13,*a*) and the welding transformer secondary (Fig. 13,*b*) are shown.



a



b

**Fig. 13.** Photographs of the discharge current welding oscillograms stored energy in capacitors: *a* – discharge current in the transformer primary  $I_{0d}$  welding; *b* – discharge current in the transformer welding transformer secondary.

The primary discharge current is less than the current in the secondary is explained by the fact that the transformer turns ratio  $n = 2$ .

Discharge current variation obtained in the two cases (with and without transformer welding transformer) show a decline big enough current and increasing the time constant of the welding transformer.

Decrease welding current and increasing time constant phenomenon is due to saturation of the transformer.

Welding transformer transfers energy to the capacitor charged to the welding device (electrodes), up to a certain value of the energy value at which the phenomenon of saturation of the core.

From this moment any increase in stored energy (increase the capacitor) is lost in heat transformer, Foucault currents etc.

The experiments demonstrate that the use of the welding transformer welding equipment with stored energy may lead to loss of performance equipment.

To eliminate or reduce this negative transformer failure it must be built to reach at least the welding equipment performance transformerless version, namely:

- replacement of permalloy core ferrite core;
  - the number of turns in the primary and the secondary has only one turn ( $n$  increasing conversion ratio).
- Before the actual welding, welding both components and electrodes must undergo preparatory operations:
- mechanical cleaning with a wire brush or sandpaper;
  - very fine finishing with sandpaper or felt, until almost metallic sheen (very low roughness);
  - degreasing with acetone, trichlorethylene etc.
  - electrodes are polished skin and fat with acetone, trichlorethylene or other degreaser.

The electrodes used in welding are made of copper stored energy by cutting the tip of tungsten and thorium.

Because high electrical resistance of tungsten, its free length was brought to zero by silvering, and brass plating.

Operations to prepare the components to be welded and the electrodes are needed because:

- a layer of oxides or other impurities enter a high electrical resistance or even the insulator;
- high roughness can lead to breakthroughs parts because the current densities are high.

Another possibility for measuring the discharge current is a magnetic core and a Hall sensor [3, 4].

A hall-effect sensor and a magnetic core are used to measure the magnetic field induced by the load current. The following figure shows the mechanical structure of the current sensing circuit.

The hall-effect sensor A1302 transforms the magnetic field into a proportional voltage signal with a resolution of  $1.3 \text{ mV/Gauss}$ . Figure 14 presents the circuit.

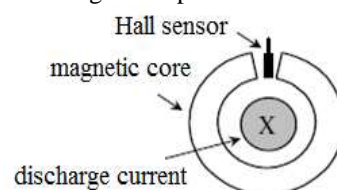


**Fig. 14.** Sensing circuit for weld current.

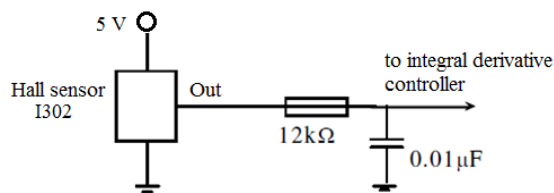


Fig. 15. Low-pass filter.



Fig. 16. Packages: *a* – 3-Pin SOT23W (suffix LH);  
*b* – 3-Pin SIP (suffix UA).

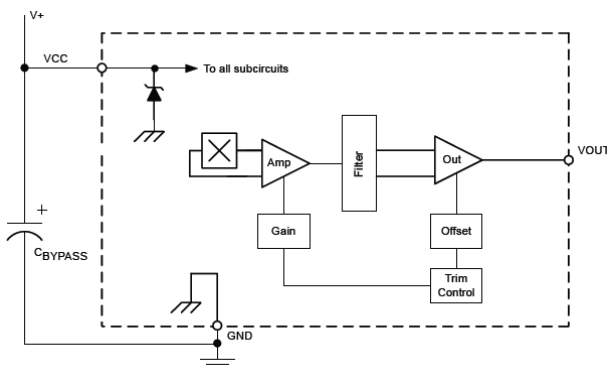


Fig. 17. Functional block diagram.

Through experimental calibration, the scaling of the current sensor is obtained as 4.6 A/mV.

The A1301 and A1302 are continuous-time, ratiometric, linear Hall-effect sensor Ics (Fig. 15) [5].

They are optimized to accurately provide a voltage output that is proportional to an applied magnetic field. These devices have a quiescent output voltage that is 50% of the supply voltage. Two output sensitivity options are provided: 2.5 mV/G typical for the A1301, and 1.3 mV/G typical for the A1302.

The Hall-effect integrated circuit included in each device includes a Hall circuit, a linear amplifier, and a CMOS Class A output structure. Integrating the Hall circuit and the amplifier on a single chip minimizes many of the problems normally associated with low voltage level analogue signals.

High precision in output levels is obtained by internal gain and offset trim adjustments made at end-of-line during the manufacturing process.

These features make the A1301 and A1302 ideal for use in position sensing systems, for both linear target motion and rotational target motion. They are well-suited

for industrial applications over extended temperature ranges, from  $-40^{\circ}\text{C}$  to  $125^{\circ}\text{C}$ .

Two device package types are available (Fig. 16): LH, a 3-pin SOT23W type for surface mount, and UA, a 3-pin ultramini SIP for through-hole mount. They are lead (Pb) free (suffix,  $-T$ ) with 100% matte tin plated leadframes.

The functional block diagram is shown in Fig. 17.

## CONCLUSIONS

Welding equipment in points with stored energy electrostatic field allowing:

- precise metering of energy at welds and heat concentration in the desired region in a very short time;
- welding material alloys and high thermal conductivity;
- welding materials and alloys of different nature which occurs at the point welded alloy is very small homogeneous;
- determination of energy at the weld energy to produce no breakthroughs in thin pieces.

It saves electricity because charging the battery energy (capacitors) requires low power to the grid, this relatively long loading time due to the time of discharge capacitors (of the order of microseconds).

The role of the welding transformer welding equipment stored energy is to increase the welding current and to protect the operator from electrical shock.

Transformer welding equipment can decrease performance.

Reducing or eliminating the influence of the welding transformer must be replaced permalloy core ferrite core and increasing ratio of transformation.

Welding electrodes using stored energy in capacitors are copper core length and free of thorium wolfram zero.

Given the transitory nature and high values of the discharge current kA can use a coil-type transducer Rogowski or a magnetic core and a Hall transducer.

## REFERENCES

- [1] W. Li, S. J. H, and J. Ni, *On-line quality estimation in resistance spot welding*, Journal of Manufacturing Science and Engineering, Transaction of the ASME, Vol. 122, 2000.
- [2] Practical Aspects of Rogowski Coil Applications to Relaying IEEE Power Engineering Society Special report September 2010.
- [3] Jin Lin, *Power Supply designed for Small Scale Resistance Spot Welding*, Thesis, ECE department, UWO, 2005.
- [4] L. J. Brown and J. Bai, *Improved Consistency for Resistance Spot Welding via Power Supply Control Strategy*, Material Science and Technology conference (MS&T'08) 2008.
- [5] A1301 and A1302 Continuous-Time Ratiometric Linear Hall Effect Sensor Ics, Copyright ©2005-2015, Allegro MicroSystems, LLC.